Zn^{2+} inhibition of recombinant $GABA_A$ receptors: an allosteric, state-dependent mechanism determined by the γ-subunit

K. J. Gingrich *† and P. M. Burkat †

*Departments of *Anesthesiology, and †Pharmacology and Physiology, University of Rochester, School of Medicine, 601 Elmwood Avenue, Rochester, NY, 14642, USA*

(Received 30 May 1997; accepted after revision 29 September 1997)

1. The γ-subunit in recombinant γ-aminobutyric acid ($GABA_A$) receptors reduces the sensitivity of GABA-triggered Cl^- currents to inhibition by Zn^{2+} and transforms the apparent mechanism of antagonism from non-competitive to competitive. To investigate underlying receptor function we studied Zn^{2+} effects on macroscopic and single-channel currents of recombinant $\alpha1\beta2$ and $\alpha1\beta2\gamma2$ receptors expressed heterologously in HEK-293 cells using the patch-clamp technique and rapid solution changes.

2. Zn^{2+} present for > 60 s (constant) inhibited peak, GABA (5 μM)-triggered currents of $\alpha1\beta2$ receptors in a concentration-dependent manner (inhibition equation parameters: concentration at half-amplitude (IC_{50}) = 0·94 μM; slope related to Hill coefficient, S = 0·7) that was unaffected by GABA concentration. The $\gamma2$ subunit ($\alpha1\beta2\gamma2$ receptor) reduced Zn^{2+} sensitivity more than fiftyfold (IC_{50} = 51 μM, S = 0·86); increased GABA concentration (100 μM) antagonized inhibition by reducing apparent affinity (IC_{50} = 322 μM, S = 0·79). Zn^{2+} slowed macroscopic gating of $\alpha1\beta2$ receptors by inducing a novel slow exponential component in the activation time course and suppressing a fast component of control desensitization. For $\alpha1\beta2\gamma2$ receptors, Zn^{2+} accelerated a fast component of apparent desensitization.

3. Zn^{2+} preincubations lasting up to 10 s markedly increased current depression and activation slowing of $\alpha1\beta2$ receptors, but had little effect on currents from $\alpha1\beta2\gamma2$ receptors.

4. Steady-state fluctuation analysis of macroscopic $\alpha1\beta2\gamma2$ currents (n = 5) resulted in control (2 μM GABA) power density spectra that were fitted by a sum of two Lorentzian functions (relaxation times: 37 ± 5·6 and 1·41 ± 0·15 ms, means ± S.E.M.). Zn^{2+} (200 μM) reduced the total power almost sixfold and accelerated the slow (23 ± 2·8 ms, P < 0·05) without altering the fast (1·40 ± 0·16 ms) relaxation time. The ratio (fast/slow) of Lorentzian areas was increased by Zn^{2+} (control, 3·39 ± 0·55; Zn^{2+}, 4·9 ± 0·37, P < 0·05).

5. Zn^{2+} (500 μM) depression of previously activated current amplitudes (% control) for $\alpha1\beta2\gamma2$ receptors was independent of GABA concentration (5 μM, 13·2 ± 0·72%; 100 μM, 12·2 ± 2·9%, P < 0·8, n = 5). Both onset and offset inhibition time courses were biexponential. Onset rates were enhanced by Zn^{2+} concentration. Inhibition onset was also biexponential for preactivated $\alpha1\beta2$ receptors with current depression more than fourfold less sensitive (5 μM GABA, IC_{50} = 3·8 μM, S = 0·84) relative to that in constant Zn^{2+}.

6. The results lead us to propose a general model of Zn^{2+} inhibition of $GABA_A$ receptors in which Zn^{2+} binds to a single extracellular site, induces allosteric receptor inhibition involving two non-conducting states, site affinity is state-dependent, and the features of state dependence are determined by the γ-subunit.

γ-Aminobutyric acid (GABA) is the primary inhibitory neurotransmitter in the vertebrate central nervous system. GABA binding to $GABA_A$ receptors activates an integral Cl^- channel that results in membrane hyperpolarization and suppressed neuronal excitability. $GABA_A$ receptors are putative heteropentamers composed of protein subunits from five distinct classes (α, β, γ, δ, and ϵ). The resultant structural diversity is significant, since the properties of

heterologously expressed channels are critically dependent on subunit combination (Levitan *et al.* 1988; Verdoorn, Draguhn, Ymer, Seeburg & Sakmann, 1990; Sigel, Baur, Mohler & Malherbe, 1990).

Zn^{2+} is a trace metal that is differentially distributed in the central nervous system. Zn^{2+} modulates synaptic transmission (Westbrook & Mayer, 1987; Xie & Smart, 1991; Zhou & Hablitz, 1993) and specifically inhibits GABA-triggered Cl^- fluxes of $GABA_A$ receptors (Westbrook & Mayer, 1987; Smart & Constanti, 1990; Legendre & Westbrook, 1991; Celentano, Gyenes, Gibbs & Farb, 1991; Smart, 1992). This may have meaningful functional consequences since Zn^{2+} is found in vertebrate synaptic vesicles (Haug, 1967; Perez-Clausell & Danscher, 1985), released by synaptic activation (Howell, Welch & Frederickson, 1984; Aniksztejn, Charlton & Ben-Ari, 1987) and may reach local concentrations of hundreds of micromoles per litre (Assaf & Chung, 1984; Frederickson & Moncrieff, 1994).

The sensitivity of native $GABA_A$ receptors to Zn^{2+} inhibition is diverse. Inhibition is observed in lobster muscle (Smart & Constanti, 1982) and cultured hippocampal neurons (Westbrook & Mayer, 1987; Mayer & Vyklicky, 1989), but not in dorsal horn interneurons (Curtis & Gynther, 1987). Studies of recombinant receptors indicate this diversity is determined by subunit composition where the presence of the γ-subunit leads to relative insensitivity (Draguhn, Verdoorn, Ewert, Seeburg & Sakmann, 1990; Smart, Moss, Xie & Huganir, 1991). The insensitivity of γ-subunit-containing receptors is further moderated by coexpression with δ-subunits (Saxena & Macdonald, 1994) or by variation in the α-subunit type ($\alpha1$ *vs.* $\alpha2$ or $\alpha3$) (White & Gurley, 1995).

The mechanism of antagonism is also variable. Inhibition of GABA-triggered currents in native $GABA_A$ receptors appears competitive in dorsal root ganglion (Akaike, Yakushiji, Tokutomi & Carpenter, 1987; Yakushiji, Tokutomi, Akaike & Carpenter, 1987) and spinal cord (Celentano *et al.* 1991). However, the apparent mechanism is non-competitive in hippocampus and rat superior cervical ganglion (Westbrook & Mayer, 1987; Mayer & Vyklicky, 1989; Smart & Constanti, 1990; Legendre & Westbrook, 1991). Recombinant studies suggest the γ-subunit also influences the apparent mechanism of inhibition such that $\alpha\beta$ receptors manifest non-competition (Draguhn *et al.* 1990; Smart *et al.* 1991) and $\alpha\beta\gamma$ receptors display competition (Chang, Amin & Weiss, 1995; for review, see Smart, Xie & Krishek, 1994).

It is likely that Zn^{2+} binds to a distinct extracellular site, allosterically triggering transition to a long-lived, non-conducting state (Celentano *et al.* 1991; Smart, 1992; White & Gurley, 1995). This reconciles a number of consistent observations made in native and recombinant receptors: weak voltage dependence (Westbrook & Mayer, 1987; Mayer & Vyklicky, 1989; Draguhn *et al.* 1990; Smart & Constanti, 1990; Legendre & Westbrook, 1991; Celentano *et al.* 1991), little or no change in single-channel properties (Draguhn *et al.* 1990; Legendre & Westbrook, 1991; Smart, 1992), and an extracellular site that is distinct from GABA, barbiturates, benzodiazepines, steroids and picrotoxin sites (Legendre & Westbrook, 1991; Celentano *et al.* 1991; Smart, 1992). However, this model of inhibition cannot account for the variety observed in the mechanism of antagonism. Therefore, either key features of a general model are missing, or none exist owing to differences in fundamental function resulting from changeable subunit composition. To explore this issue, we investigated the effects of Zn^{2+} on macroscopic and single-channel, GABA-triggered, Cl^- currents of recombinant receptors composed of $\alpha1\beta2$ and $\alpha1\beta2\gamma2$ subunits; these receptors manifest apparent non-competitive and competitive inhibition, respectively. Receptors resulted from transient transfection with combinations of cDNAs encoding rat brain $GABA_A$ receptors subunits of HEK-293 cells. Rapid solution changes (Gingrich, Roberts & Kass, 1995) provided for the study of changes in macroscopic gating.

In this study, Zn^{2+} induced distinct effects on current magnitude and gating in $GABA_A$ receptors that differed in the $\gamma2$-subunit. We considered explicit gating models to account for the empirical observations. The results lead us to propose a general model of Zn^{2+} inhibition of $GABA_A$ receptors that includes a single extracellular site, receptor inhibition involving two allosteric kinetically distinct non-conducting states, and state-dependent affinity with features determined by the γ-subunit. A preliminary report of this work has appeared in abstract form (Burkat, Roberts & Gingrich, 1995).

METHODS

Cell culture and transient transfection

Transformed HEK-293 cells, purchased from ATCC (Bethesda, MD, USA) or generously provided by Dr Robert Kass, Department of Pharmacology, Columbia University (New York, NY, USA) were plated onto fibronectin (Sigma)-coated plastic coverslips (Nunc, Inc., Naperville, IL, USA) and cultured in minimum essential medium (MEM) supplemented with 10% fetal calf serum, 1% glutamine, 1% penicillin, and 1% streptomycin (all Gibco). Following incubation in 5% CO_2 for 48–72 h, cells were transiently transfected using a lipofection technique previously described (Gingrich *et al.* 1995) with cDNAs encoding rat brain $\alpha1$, $\beta2$, and $\gamma2$ subunits inserted individually into the plasmid pCDM8 (Invitrogen, Carlsbad, CA, USA). Briefly, aliquots of the lipofection reagent (Lipofectamine, Gibco), and appropriate plasmids were mixed in a modified serum-free medium (Optimem, Gibco) and incubated for 10 min. Transfections were based on equal weights of total DNA. t-Antigen was coexpressed with $\alpha1$ and $\beta2$ to enhance expression. Cells were washed and serum-containing medium was replaced with Optimem, followed by addition of liposome–plasmid-containing solution. After a 16–18 h incubation period (37 °C, 5% CO_2), the cells were washed and returned to serum-containing MEM for further incubation. Cells were ready for electrophysiological studies approximately 48 h after transfection. To address the possibility that HEK-293 cells may constitutively

express $GABA_A$ receptor subunits, we transfected our cell line with α1- or β2-subunits alone. No detectable GABA-triggered currents were elicited from single cells, ruling out the possibility of significant constitutive production of α, β, or γ subunits since $\alpha\beta$ and $\alpha\gamma$ combinations express robustly (Verdoorn *et al.* 1990).

Electrophysiology

Coverslips with transfected cells were transferred to a modified culture dish mounted on the stage of an Olympus IMT-2 inverted microscope with Hoffman modulated optics. The cells were immersed in a modified Tyrode solution containing (mM): 135 NaCl, 5·4 KCl, 1 $MgCl_2$, 5 Hepes (pH 7·3). The pipette solution consisted of (mM): 140 CsCl, 1 $MgCl_2$, 11 EGTA, 10 Hepes (pH 7·3). Currents were recorded with whole-cell and outside-out configurations of the patch clamp (Hamill, Marty, Neher, Sakmann & Sigworth, 1981) using an Axopatch 200A (Axon Instruments) amplifier. Macroscopic currents (−60 mV) were filtered at 1 kHz (−3 dB, 4-pole Bessel) and sampled at 1–2 kHz. Single-channel currents from outside-out patches (−50 mV) were filtered at 1 kHz (−3 dB, 4-pole Bessel) and sampled at 5 kHz. Digitized data were collected and stored on IBM-compatible (Gateway 2000 4DX-2-66) computers running the Axobasic Environment (Axon Instruments) using software of our own design. We used single cells that were not electrically coupled to other cells as judged visually and by cell capacitance (10–20 pF, typical for individual HEK cells). Data were collected at room temperature (20–23 °C). The chloride potential is 0 mV under these ionic conditions resulting in negative currents (outward Cl^- movement) in our experiments. Zn^{2+} (0–1000 μM) was present in the bathing solution for more than 60 s before GABA application unless otherwise indicated.

Rapid solution changes

GABA (Sigma) and Zn^{2+} were applied transiently to the cells via an electro-mechanical solution changer. Control and test solutions were introduced into the lumen of dual- and triple-barrelled pipettes. A syringe pump (Harvard Instruments, Cambridge, MA, USA) determined the rate of solution perfusion. The pipette was mounted on a macro-block piezoelectric transducer (Polytec Optronics, Costa Mesa, CA, USA), which can move the pipette tip 50 μm in < 5 ms. The cell was continually perfused with control solution. Test solutions were applied by delivering the appropriate voltage pulse to the macro-block translator such that the pipette tip moved the distance between the stream centres. In this manner, test solutions containing combinations of GABA and Zn^{2+} could be pulsed on–off around a cell in < 30 ms or a cell-free patch in < 1 ms. The period of GABA application was sufficiently long to prevent accumulation of desensitized receptors (generally > 120 s). Following washout additional GABA-triggered currents were collected to exclude cells that suffered from rundown (> 10 % decline).

Fluctuation analysis of steady-state, GABA-gated currents

Steady-state, GABA-gated current noise was digitized on-line (1 kHz) after low-pass analog filtering at 500 Hz (−3db, 8-pole Bessel). Digitized records underwent digital high-pass filtering at 0·25 Hz (2-pole). Epochs of 500 ms (enabling 2 Hz resolution) were visually inspected and those with artifacts were rejected or edited accordingly. Mean spectral density of each current was calculated from fifteen to forty separate spectra. The net mean power spectrum for the GABA-gated noise was obtained by subtraction of the mean background spectrum in the absence of GABA. The manipulations of sampled data were performed using routines of our own design written in the MATLAB (Mathworks, Natick, MA, USA) environment. The net, one-sided GABA-gated spectra, were fitted with the sum of two Lorentzian components using a least-squares technique.

Data analysis

The time courses of composite activation and desensitization, inhibition onset or offset of macroscopic currents were fitted with a sum of up to three exponentials:

$$A_1 \exp(-k_1 t) + A_2 \exp(-k_2 t) + A_3 \exp(-k_3 t) + B,$$

with Origin (MicroCal, Northampton, MA, USA) using a least-squares criterion, where k_i values are estimated rates (per second). Fitting began after the initial sigmoidal foot when discernible. Multiexponential fitting allows an accurate description of current responses with rising and falling phases since both processes are addressed simultaneously and provides for analysis of dominant gating (Maconochie, Zempel & Steinbach, 1994). Inhibition concentration–response relationships were fitted with a normalized inhibition equation: $I = {IC_{50}}^S / ({IC_{50}}^S + [Zn^{2+}]^S)$ using a least-squares technique, where I is current magnitude normalized to control, IC_{50} is the half-blocking concentration and S is the slope factor related to the Hill coefficient. Results are given as means ± S.E.M. Statistical tests were Student's unpaired t tests unless otherwise specified and significance was taken as $P < 0{\cdot}05$.

Simulation of gating models and parameter estimation

Simulations of gating models utilized differential equations solved numerically using the Euler method and written in Excel (Microsoft). The sensitivity of the response to iteration time step was examined in all simulations and made sufficiently small to minimize error. The parameter estimation technique minimized a squared error performance criterion using the Levenberg–Marquardt method. The uniqueness of parameter sets was evaluated by systematically adjusting the initial parameter values before parameter estimation. In this way the performance surface was searched from different initial starting locations. A parameter set was considered unique if the final parameter values were insensitive to initial values. All programs were compiled and executed on an IBM-compatible 486 (Gateway 2000) computer.

RESULTS

The sensitivity and mechanism of antagonism of Zn^{2+} inhibition is influenced by the γ2-subunit

We first considered inhibition of peak current by Zn^{2+}. Figure 1*Aa* shows currents (activation marked by downward current deflection) over a range of Zn^{2+} concentrations triggered by GABA (5 μM) in individual cells expressing $\alpha1\beta2$ and $\alpha1\beta2\gamma2$ subunits. The dissimilar macroscopic kinetics in control (Zn^{2+}, 0 μM) document the incorporation of different subunits in these receptors (Verdoorn *et al.* 1990). Zn^{2+} inhibited peak currents of $\alpha1\beta2$ receptors in a dose-dependent fashion. Figure 1*Ac* plots the concentration–response relationship of normalized current in grouped data and the fit of these data by an inhibition equation. Comparable inhibition of $\alpha1\beta2\gamma2$ currents (Fig. 1*Ab*) required more than fiftyfold greater Zn^{2+} concentration marking strongly reduced sensitivity that is confirmed in grouped data (Fig. 1*Ac*) by a rightward shift of the fitted inhibition curve. This is in accordance with previous reports of the γ-subunit inducing relative insensitivity to Zn^{2+} (Draguhn *et al.* 1990; Smart *et al.* 1991). We next examined GABA antagonism of inhibition at a fixed Zn^{2+} concentration. Figure 1*Ba* shows currents triggered by two GABA concentrations (low, 5 μM; high, 100 μM) in control

and nearly equipotent Zn^{2+} concentrations (at 5 μM GABA) in cells expressing the indicated receptors. Depression of $\alpha1\beta2$ peak current by Zn^{2+} was unchanged by the increase in GABA concentration. This finding was reproduced in grouped data (Fig. 1*Bb*) where currents were reduced by roughly 80% independent of GABA concentration, denoting a non-competitive mechanism consistent with previous reports (Draguhn *et al.* 1990; Smart *et al.* 1991).

In contrast, Zn^{2+} inhibition of $\alpha1\beta2\gamma2$ currents was partly surmounted by the same increase in GABA concentration indicating apparent competition, which was confirmed in grouped data (Fig. 1*Bb*). Notably, high GABA concentration (5000 μM) incompletely antagonized inhibition. To characterize the mechanism of antagonism further, we re-examined the Zn^{2+} inhibition relationship but at higher GABA concentration (100 μM). This change shifted the relationship rightward indicating an apparent reduction of Zn^{2+} affinity (Fig. 1*Ac*). In addition, inhibition of current plateau (data not shown) was independent of GABA concentration (1 μM, $17 \pm 3{\cdot}4\%$ of control; 1000 μM, $24 \pm 4{\cdot}6\%$; $P < 0{\cdot}24$, $n = 5$), which indicates non-competition of receptors contributing to current at equilibrium. These observations point to apparent 'mixed antagonism' (Smart & Constanti, 1986) of $\alpha1\beta2\gamma2$ receptors, and extend previous findings of competition by Chang *et al.* (1995) in *Xenopus* oocytes. Also, the findings indicate, in the same expression system, that the $\gamma2$-subunit determines the apparent mechanism of antagonism for peak current.

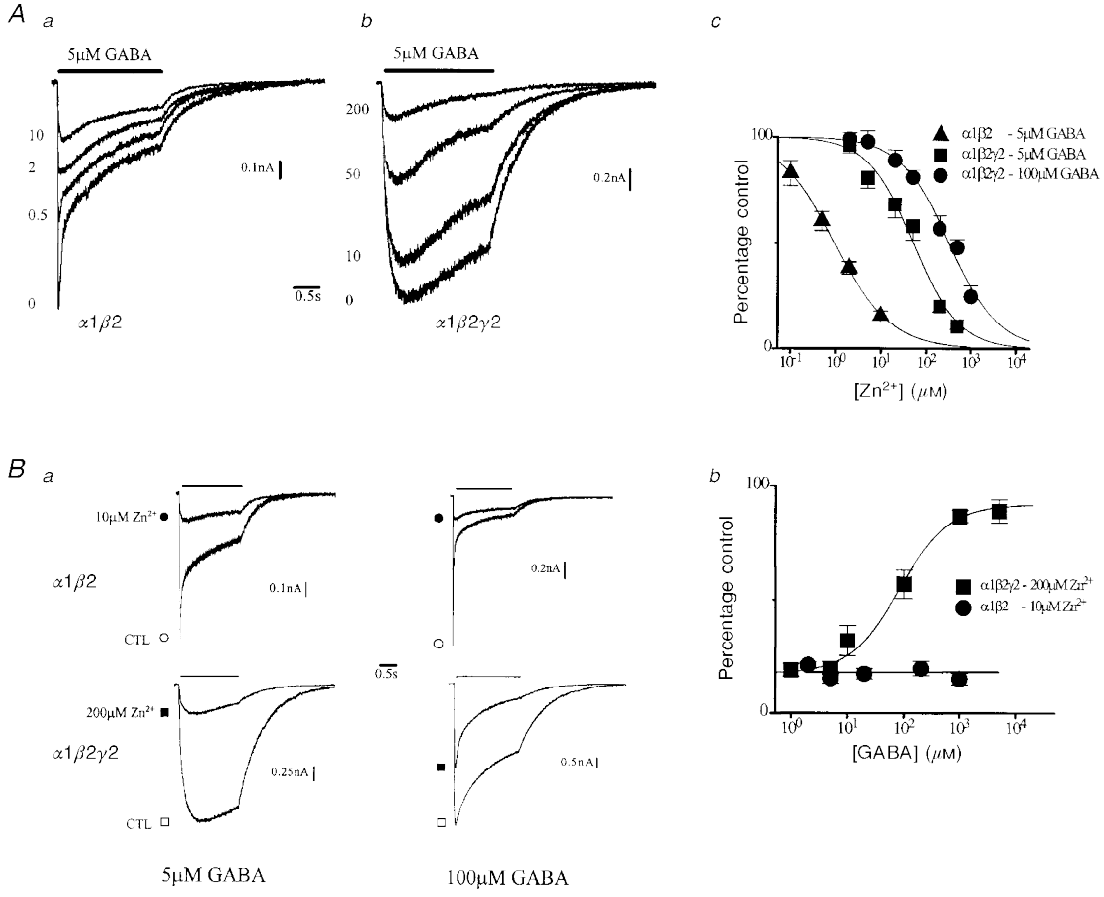

Figure 1. Zn^{2+} inhibition of peak current

Aa and *b*, macroscopic currents triggered by GABA (5 μM, filled bar) in the presence of a range of Zn^{2+} concentrations (in μM; left of trace) for individual cells expressing $\alpha1\beta2$ and $\alpha1\beta2\gamma2$ subunits. Downward current deflection reflects receptor opening. GABA was applied using rapid solution changes. *c*, inhibition curves were constructed by plotting peak current as percentage of control *versus* Zn^{2+} concentration (generally $n = 6$). Smooth curves are least-squares fits of the inhibition equation (see Methods). Fitted parameters are: $\alpha1\beta2$ (5 μM GABA), $IC_{50} = 0{\cdot}94$ μM, $S = 0{\cdot}70$; $\alpha1\beta2\gamma2$ (5 μM GABA), $IC_{50} = 51$ μM, $S = 0{\cdot}86$; $\alpha1\beta2\gamma2$ (100 μM GABA), $IC_{50} = 322$ μM, $S = 0{\cdot}79$. *Ba*, currents triggered by application (bars) of different GABA concentrations in the absence (CTL, open symbols) and presence (filled symbols) of Zn^{2+} concentrations from individual cells expressing indicated receptors. *b*, peak current (percentage of control) concentration–response relationships for GABA at a fixed Zn^{2+} concentration ($n = 5$). Continuous lines were drawn by hand.

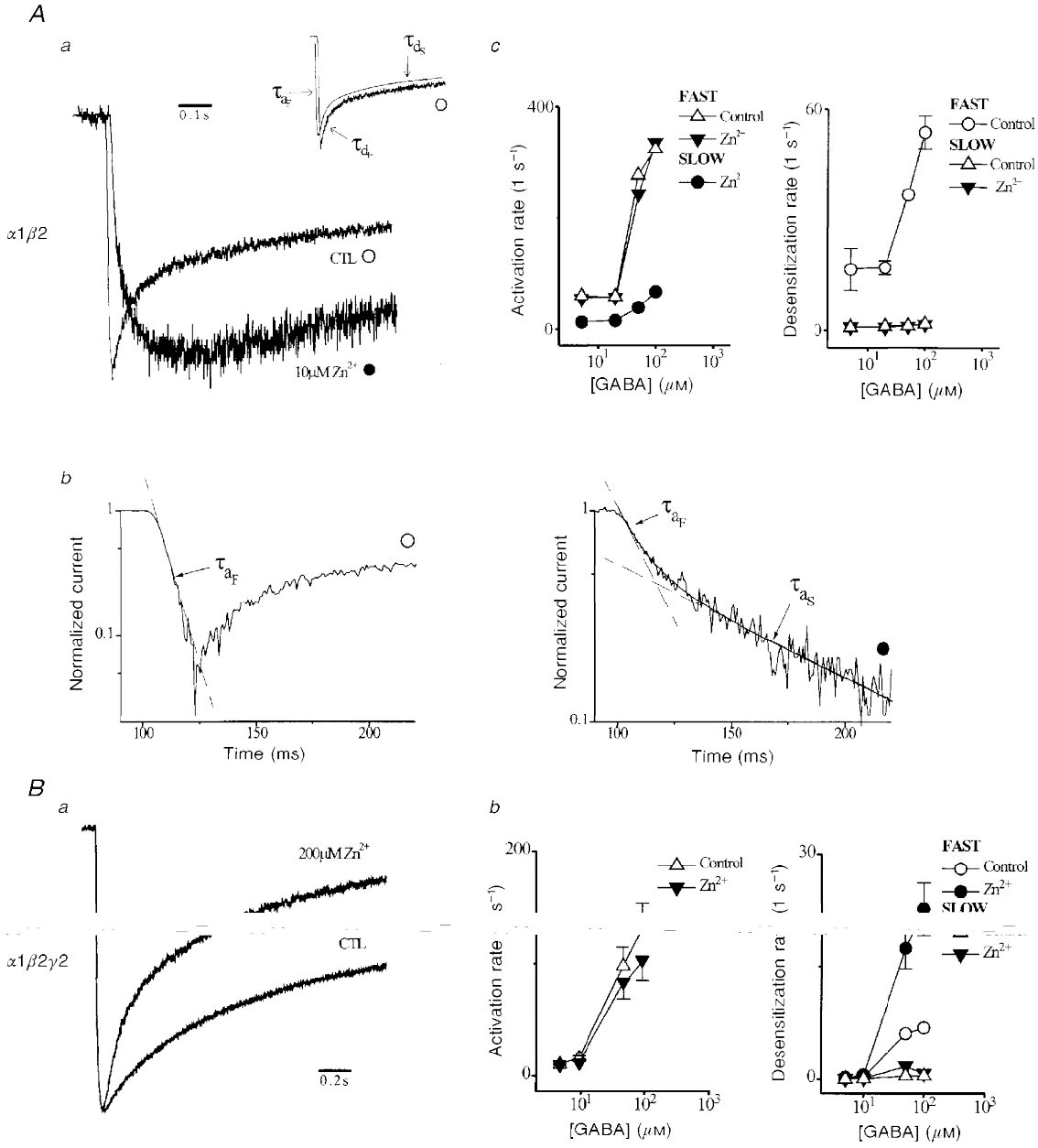

Figure 2. Zn^{2+} effects on macroscopic gating

Aa, normalized $\alpha1\beta2$ responses (5 μM GABA) replotted from Fig. 1*B* to illustrate the effects of Zn^{2+} on macroscopic current kinetics. Zn^{2+} response was rightward shifted to permit clear observation of activation time course. Inset, plot of control response and triexponential function fit (smooth line, shifted for clarity). Exponential components are indicated by their respective time constants (fast activation, τ_{a_F}; fast, τ_{d_F}, and slow, τ_{d_S} densensitization). Time constants (τ) are the reciprocal of associated rates (k). Fitted parameters are: $A_{a_F} = 1{\cdot}2$ nA, $k_{a_F} = 108\ s^{-1}$, $A_{d_F} = -0{\cdot}81$ nA, $k_{d_F} = 33{\cdot}3\ s^{-1}$, $A_{d_S} = -0{\cdot}33$ nA, $k_{d_S} = 2{\cdot}48\ s^{-1}$, $B = -0{\cdot}42$ nA. *Ac*, GABA concentration dependence of activation and desensitization rates from fitted triexponential functions (generally $n = 5$ cells). *Ab*, semilogarithmic plots of currents normalized to peak current. Control (○) activation is described by a single fast exponential (dashed line, time constant, τ_{a_F}). Zn^{2+} (●) adds a second slow exponential component to activation (time constant, τ_{a_S}). The sum of these exponentials (continuous line) describes the activation time course. *Ba*, normalized $\alpha1\beta2\gamma2$ responses (100 μM GABA) replotted from Fig. 1*B* to illustrate the effects of Zn^{2+} on macroscopic current kinetics. *Bb*, GABA concentration dependence of activation and desensitization rates from fitted triexponential functions (generally $n = 5$ cells).

Zn^{2+} induces distinct effects on macroscopic gating of $\alpha1\beta2$ and $\alpha1\beta2\gamma2$ receptors

We used rapid solution changes (< 30 ms), which permit kinetic analysis of gating manifest in macroscopic currents (Maconochie *et al.* 1994; Gingrich *et al.* 1995). Figure 1*A* shows that Zn^{2+} slowed $\alpha1\beta2$ apparent desensitization in a dose-dependent fashion, while $\alpha1\beta2\gamma2$ gating changed little except at high concentrations where desensitization appeared slightly accelerated. These divergent observations prompted us to investigate gating effects. Figure 2*Aa* shows $\alpha1\beta2$ responses (5 μM GABA) from Fig. 1*B* replotted after normalizing by peak current. The control current (CTL) exhibited rapid activation resulting in an early current peak, followed by biphasic desensitization. To characterize the dominant gating, we fitted multiexponential functions to current time courses (Maconochie *et al.* 1994). The inset in Fig. 2*Aa* shows that the control response is well described by a triexponential function (smooth line) composed of a rising and two falling components that represent activation and desensitization, respectively. These components are recognizable as individual phases and are labelled with associated exponential time constants. Zn^{2+} markedly alters the time course by slowing activation and apparent desensitization. Closer inspection of the Zn^{2+} response, shifted for clarity, reveals a biphasic activation time course. Figure 2*Ab* plots normalized currents on a semilogarithmic scale to examine the kinetic nature of the activation time course. The left panel shows that control activation is well described by a single fast exponential function. The right panel shows that Zn^{2+} alters activation by introducing a new slow exponential component. The sum of these two exponential functions (smooth line) closely accounts for the activation time course. The entire Zn^{2+} response was well fitted by a triexponential function composed of the two activation components and a single slow desensitization component (not shown).

To examine the interaction of inhibition and gating we plotted fitted kinetic parameters *versus* GABA concentration (Fig. 2*Ac*). Figure 2*Ac* plots rates of activation (fast and slow) and desensitization in grouped data. In control, activation and desensitization were enhanced by GABA (Maconochie *et al.* 1994). In control and Zn^{2+}, the fast rates of activation and the slow components of desensitization were similarly dependent on GABA. The slow, Zn^{2+}-induced rate of activation was more than fivefold less than the fast, and was augmented by GABA. The results are consistent with two discrete populations of resting receptors in Zn^{2+}. One is probably Zn^{2+} free, which activates normally, and the other Zn^{2+} bound, which activates slowly. In turn, slowing of apparent desensitization may be explained by a reduction in the probability of states that experience desensitization. Alternatively, Zn^{2+} may rapidly interact with ligand-bound, closed receptors before opening during activation. However, this mechanism seems unlikely to account for non-competition. More complex mechanisms may be invoked to account for these results and cannot be excluded. At a simple level, the data are consistent with primary inhibition of resting $\alpha1\beta2$ receptors.

Zn^{2+} induced different effects in $\alpha1\beta2\gamma2$ currents. Figure 2*Ba* shows $\alpha1\beta2\gamma2$ responses from Fig. 1*B* replotted after normalization, which demonstrates that Zn^{2+} accelerates apparent desensitization. We again fitted triexponential functions to the current time course. Unlike $\alpha1\beta2$ receptors, both control and Zn^{2+} responses were well fitted by a triexponential function comprised of one activation and two desensitization components (not shown). Figure 2*Bb* plots, in grouped data, rates of fast activation and desensitization (fast and slow) *versus* GABA concentration. Activation rate was reduced slightly by Zn^{2+} at high GABA concentration. Zn^{2+} enhanced apparent desensitization by increasing the fast component nearly threefold at high GABA concentration with little change in the slow component. The findings are consistent with preferential inhibition of states visited after ligand exposure.

These differential effects on receptor gating support the argument for a state-dependent, inhibitory mechanism with features determined by the $\gamma2$-subunit. For $\alpha1\beta2\gamma2$, Zn^{2+} preferentially inhibits states visited following ligand exposure. In contrast, resting $\alpha1\beta2$ receptors are primarily inhibited and must ultimately proceed to desensitized states relatively unaffected by GABA, since inhibition appears non-competitive.

Role of resting, ligand-free receptors

To investigate the role of resting $\alpha1\beta2$ receptors we examined the effects of Zn^{2+} preincubation on current magnitude and activation kinetics. Figure 3*Aa* shows a response family triggered by GABA from an individual cell expressing $\alpha1\beta2$ receptors. Bracketing control responses in the absence of Zn^{2+} are shown on the far left and right and document preparation stability. Next, six responses with different Zn^{2+} preincubation periods (time between Zn^{2+} (open bar) and GABA (filled bar) applications) are plotted on the same baseline. The first test response was induced by coapplication of GABA and Zn^{2+}, a preincubation period of zero. Peak current was reduced roughly one-third without alteration of activation kinetics (see Fig. 3*Ab*). Increasing preincubation time resulted in complex effects on current magnitude and kinetics, indicating notable interactions of Zn^{2+} with resting, ligand-free receptors. Inhibition of peak current increased markedly over the first second, and eventually reached a plateau by 5 s.

The inset in Fig. 3*A* replots four responses with different preincubation periods after magnitude normalization and alignment in time to permit comparison of activation kinetics. This shows activation kinetics were progressively slowed by increasing the preincubation period. As before, the time course was characterized by triexponential function

fitting. Figure 3*Ab* and *C* plots in grouped data, activation rates (fast and slow), the fraction of slow activation (%Slow), and fraction of inhibited receptors *versus* preincubation period. Both the number of inhibited receptors and activation kinetics varied with the preincubation period in a biphasic manner. The first phase occurred rapidly within 0·5 s, wherein the number of inhibited receptors increased considerably and monoexponential activation slowed twofold. The second phase occurred slowly over seconds. Activation kinetics became biexponential as the slow component grew in proportion. The first phase may reflect a growing number of Zn^{2+}-bound resting receptors with slowed activation unresolvable in the activation time course. With an increasing preincubation period, the number or kinetics of Zn^{2+}-bound receptors progresses until a distinct slower component and one attributable to control can be discerned; this may underlie the second phase. Preincubation periods of 10 s resulted in receptor inhibition and activation kinetics comparable with that observed in constant Zn^{2+} (see Fig. 1). We used the current inhibition response as an approximate single indicator of the overall onset kinetics of these complex effects in $\alpha1\beta2$ receptors. The time course of current inhibition was well fitted by a biexponential function (Fig. 3*C*, thick line) with fast (6·7 s^{-1})

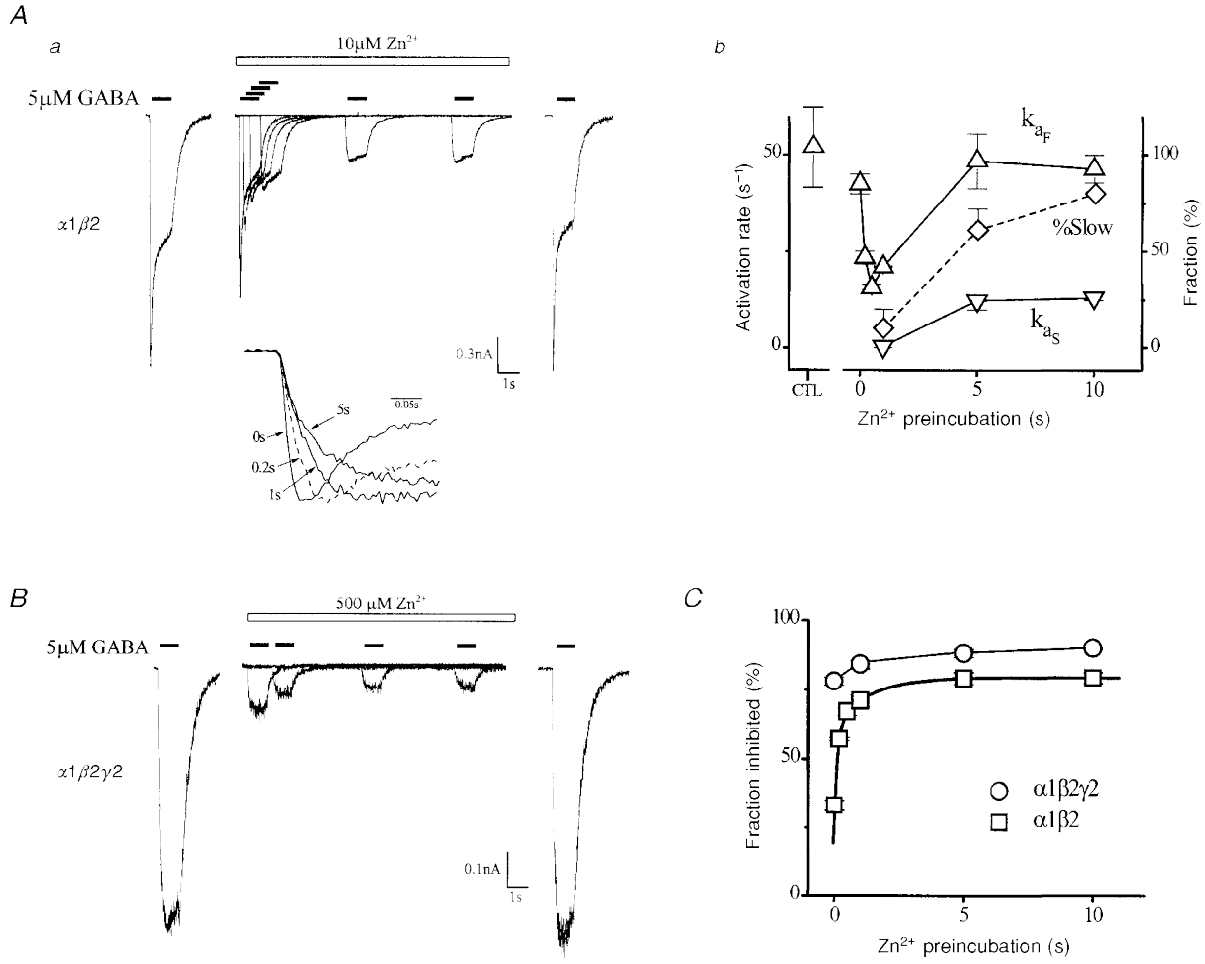

Figure 3. Effects of Zn^{2+} preincubation on current magnitude and kinetics

Aa, currents triggered by GABA (5 μM, filled bars) from a single cell expressing $\alpha1\beta2$ receptors with differing periods of Zn^{2+} preincubation. An initial control response is displayed on the extreme left. Shown next on the same baseline are responses over a range of Zn^{2+} preincubation periods (time difference between Zn^{2+} (10 μM, open bar) and GABA applications). A final bracketing control response is shown on the extreme right. Inset shows four normalized responses aligned in time on an expanded time scale with indicated preincubation periods. *Ab*, plots of activation parameters derived from multiexponential fitting. Plotted parameters include fast (k_{a_F}) and slow (k_{a_S}) activation rates, and fraction of activation time course that is slow (%Slow). *B*, same protocol as in *Aa* applied to a single cell expressing $\alpha1\beta2\gamma2$ receptors (5 μM GABA, 500 μM Zn^{2+}). *C*, fractional inhibition of current magnitude *versus* Zn^{2+} preincubation in cells expressing $\alpha1\beta2$ and $\alpha1\beta2\gamma2$ receptors as indicated ($n = 3$–7 cells). Thick smooth curve is a biexponential function fit of $\alpha1\beta2$ response (parameters: $A_F = -0{\cdot}31$, $k_F = 6{\cdot}7\ s^{-1}$, $A_S = -0{\cdot}17$, $k_S = 0{\cdot}72\ s^{-1}$, and $B = 0{\cdot}79$).

and slow ($0{\cdot}72\ s^{-1}$) rates. The data indicate that Zn^{2+} interactions with resting states play a primary role in $\alpha1\beta2$ receptor inhibition and involve two kinetically distinct components.

We next examined the effects of Zn^{2+} preincubation on $\alpha1\beta2\gamma2$ receptors using a nearly equipotent concentration (see Fig. 1). Figure 3*B* shows a response family elicited from an individual cell expressing $\alpha1\beta2\gamma2$ receptors using the same preincubation protocol. A majority of current depression occurred with Zn^{2+} coapplication without changes in gating. Longer preincubations induced little change in current magnitude (Fig. 3*C*) and kinetics. These data suggest Zn^{2+} interacts principally with ligand-bound $\alpha1\beta2\gamma2$ receptors.

Zn^{2+} affects microscopic gating of $\alpha1\beta2\gamma2$ receptors

We tested for changes in single-channel properties of ligand-exposed $\alpha1\beta2\gamma2$ receptors. To investigate microscopic gating we performed fluctuation analysis of steady-state, macroscopic currents (Neher & Stevens, 1977). The resulting power density spectra were fitted with the sum of two Lorentzian functions. Mean relaxation time constants derived from corner frequencies were $1{\cdot}41 \pm 0{\cdot}15$ and $37 \pm 5{\cdot}6$ ms for control currents (Fig. 4*A*), consistent with previous reports (Verdoorn *et al.* 1990). The addition of 200 μM Zn^{2+} reduced total power about sixfold (Fig. 4*B*) and significantly reduced the slow time constant ($23 \pm 2{\cdot}8$ ms, $P < 0{\cdot}05$, $n = 6$) without affecting the fast time constant ($1{\cdot}40 \pm 0{\cdot}16$ ms). The relative contributions were calculated from the ratio of the areas under the two Lorentzian fuctions (A_{fast}/A_{slow}). These were $3{\cdot}4 \pm 0{\cdot}55$ for currents triggered by GABA alone, consistent with results reported by Puia *et al.* (1990), and $4{\cdot}9 \pm 0{\cdot}37$ in Zn^{2+}, which are significantly different ($P < 0{\cdot}05$). Hence, the receptors contributing to the current remaining in Zn^{2+} sustained acceleration and suppression of the slow component of the open–closed gating properties. These results are in accord with those from cultured rat neurons (Smart, 1992). The change in the slow time constant indicates that Zn^{2+} induces closures with a rate in the order of $10\ s^{-1}$ and is consistent with selective inhibition of ligand-exposed receptors. We also tested whether Zn^{2+} altered measured unitary conductance. The primary single-channel conductance was derived from single-channel currents triggered (GABA, 2 μM) in outside-out, cell-free patches. At −50 mV, primary channel conductance was unchanged ($P < 0{\cdot}22$, $n = 5$ patches) from control ($29{\cdot}8 \pm 0{\cdot}21$ pS) to 100 μM Zn^{2+} ($30{\cdot}2 \pm 0{\cdot}32$ pS).

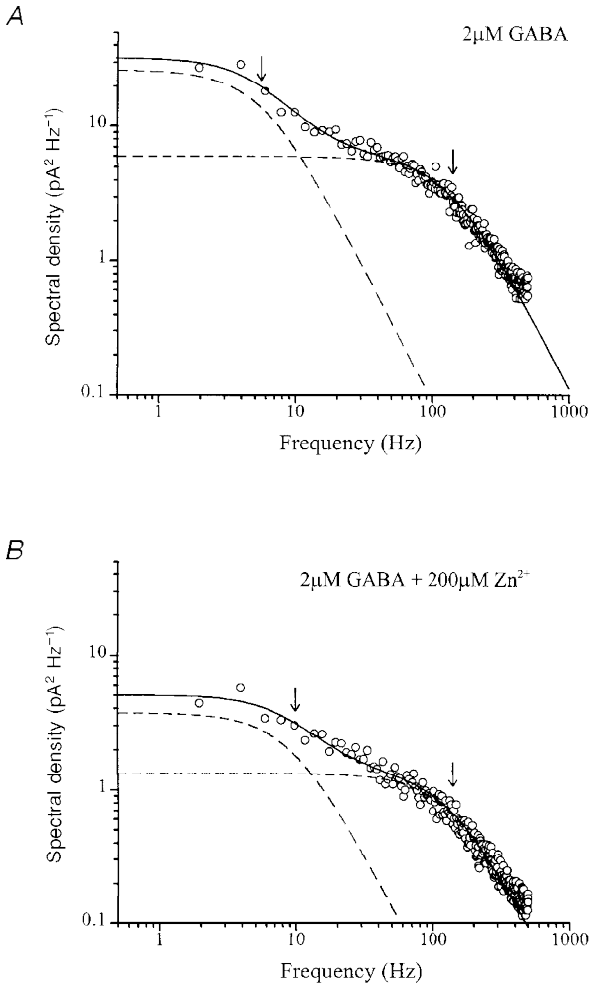

Figure 4. Zn^{2+} effects on macroscopic current fluctuations of $\alpha1\beta2\gamma2$ receptor

A, power density spectrum of steady-state macroscopic current activated by 2 μM GABA from a single cell expressing $\alpha1\beta2\gamma2$ subunits. Smooth continuous curve represents the sum of two individual Lorentzian functions (dashed lines) with corner frequencies of 5·8 and 137 Hz (arrows). *B*, power density spectrum of steady-state macroscopic current activated by 2 μM GABA in the presence of 200 μM Zn^{2+} from the same cell. Corner frequencies are 9·6 and 136 Hz (arrows).

Zn^{2+} inhibition of $\alpha1\beta2\gamma2$ currents previously activated by GABA is non-competitive

The results suggest that Zn^{2+} preferentially inhibits $\alpha1\beta2\gamma2$ states visited following ligand exposure. A state-dependent mechanism accounts for mixed antagonism of peak current through interplay between the kinetics of inhibition and activation. Low GABA concentrations induce slow activation, allowing extensive receptor inhibition before opening, and substantial depression of peak current. High GABA concentrations accelerate activation, causing greater receptor opening before inhibition, and thereby lessening depression of peak current. Inhibition after current peak enhances apparent desensitization (Fig. 2*B*). We tested whether the sensitivity of previously activated receptors is independent of GABA concentration as predicted by this mechanism. Figure 5*Aa* shows currents triggered by low (5 μM, left) and high (100 μM, middle) GABA concentrations in the same cell expressing $\alpha1\beta2\gamma2$ receptors. Scaling was adjusted to align current magnitudes at the start of inhibition. Application of 500 μM Zn^{2+} after preactivation by low GABA markedly inhibited current magnitude. The time course is biphasic and reaches a near-plateau during the 3 s application. Within 1 s of Zn^{2+} washout, control and test currents superimpose indicating that underlying native gating is unaffected. Remarkably, at high [GABA], the relative magnitude of current inhibition by the same Zn^{2+} concentration is similar (Fig. 5*Aa*, middle) marking non-competition. Lower Zn^{2+} concentration (50 μM) lessened inhibition in a dose-dependent fashion (Fig. 5*Aa*, middle). The magnitude of inhibition was computed from the difference between control and Zn^{2+} current responses at the end of the 3 s application and normalized by control. We found in grouped data, inhibition (% of control) at two Zn^{2+} concentrations was not influenced by GABA concentration (50 μM Zn^{2+}: 5 μM GABA, 40 $\pm$ 8·7 %; 100 μM GABA, 47 $\pm$ 5·3 %, $P < 0{\cdot}4$; and 500 μM Zn^{2+}: 5 μM GABA, 13·0 $\pm$ 0·72 %; 100 μM GABA, 12·2 $\pm$ 2·9 %, $P < 0{\cdot}8$, $n = 5$) demonstrating non-competition of preactivated $\alpha1\beta2\gamma2$ receptors. Figure 5*Aa*, right panel, plots the inhibition concentration–response relationship at high [GABA] and the fit (continuous line) of the inhibition equation. This relationship is similar to that in constant Zn^{2+} triggered by 5 μM GABA (Fig. 1*A*). These results are in accord with apparent mixed antagonism arising from preferential inhibition of ligand-exposed $\alpha1\beta2\gamma2$ receptors.

We next examined Zn^{2+} sensitivity of preactivated $\alpha1\beta2$ receptors. The same protocol was applied to a single cell expressing $\alpha1\beta2$ receptors (Fig. 5*B* left). Zn^{2+} induced concentration-dependent current reductions with features roughly similar to $\alpha1\beta2\gamma2$ receptors but at approximately tenfold lower concentration. Notably, the inhibition relationship fit of grouped data (Fig. 5*B* right) indicates fourfold less sensitivity compared with inhibition arising from Zn^{2+} presentation to resting $\alpha1\beta2$ receptors (see Fig. 1*A*). The results suggest state-dependent Zn^{2+} inhibition of $\alpha1\beta2$ receptors.

Inhibition of preactivated receptors involves two kinetically distinct non-conducting states

To analyse inhibition kinetics we replotted onset time courses for $\alpha1\beta2\gamma2$ receptors from Fig. 5*Aa* after normalizing for the magnitude of inhibition (Fig. 5*Ab*, left). The control time course exhibits current decay reflecting desensitization. Zn^{2+} enhanced the rate of current decay due to receptor inhibition. The time course was well fitted by a triexponential function. The inset in Fig. 5*Ab* replots the Zn^{2+} response (500 μM) on a semilogarithmic scale after normalization for current magnitude. The three exponential components appear as linear phases of the response, which are marked by dashed straight lines and labelled with associated exponential time constants. The slowest component was considered desensitization since its time constant (τ_d) is comparable with that of control decay. The two faster components were presumed to reflect the onset of inhibition and are referred to as fast and slow inhibition onset (time constants, τ_{on_F} and τ_{on_S}, respectively). Therefore, inhibition of preactivated $\alpha1\beta2\gamma2$ receptors involves two kinetically distinct components. We also examined the kinetics of inhibition onset for $\alpha1\beta2$ receptors; The inset in Fig. 5*Ba* shows it is also biexponential.

We next characterized the kinetics of Zn^{2+} inhibition for $\alpha1\beta2\gamma2$ receptors. Figure 5*Ab*, right panel, shows the concentration–response relationships for onset rates (k_{on_S} and k_{on_F}) and the fast fraction (% Fast). Onset rates differ in magnitude nearly tenfold and Zn^{2+} enhances both. Zn^{2+} also increased the contribution of the fast component. We next considered the time course of inhibition offset. Offset time courses were well fitted by a triexponential function as with inhibition onset. Figure 5*Ac*, left panel, shows offset time courses replotted from Fig. 5*Aa* (symbols identify traces), shifted to align currents at the end of the Zn^{2+} application (open bar). Continuous lines represent triexponential function fits with exponential phases labelled with the associated time constants. As for onset, the slow component is comparable with control desensitization (τ_d). The two faster components describe inhibition offset and are referred to as fast and slow offset (time constants, τ_{off_F} and τ_{off_S}, respectively). Inhibition recovery is represented by the sum of these two exponential components. The inset in Fig. 5*Ac* shows the early time course, which reflects primarily inhibition offset after normalizing for peak current on an expanded time scale. The low and high [Zn^{2+}] responses nearly superimpose, indicating offset kinetics are affected little by Zn^{2+} concentration. Figure 5*Ac*, right panel, plots the associated offset rates (k_{off_S} and k_{off_F}) and the fast fraction (% Fast) *versus* Zn^{2+} concentration. These data confirm that offset kinetics are mostly independent of Zn^{2+} concentration. Similar qualitative observations of the inhibition time course can be made from the responses of comparable experiments by Mayer & Vyklicky (1989) in cultured hippocampal neurons (see their Fig. 4*A* and *B*).

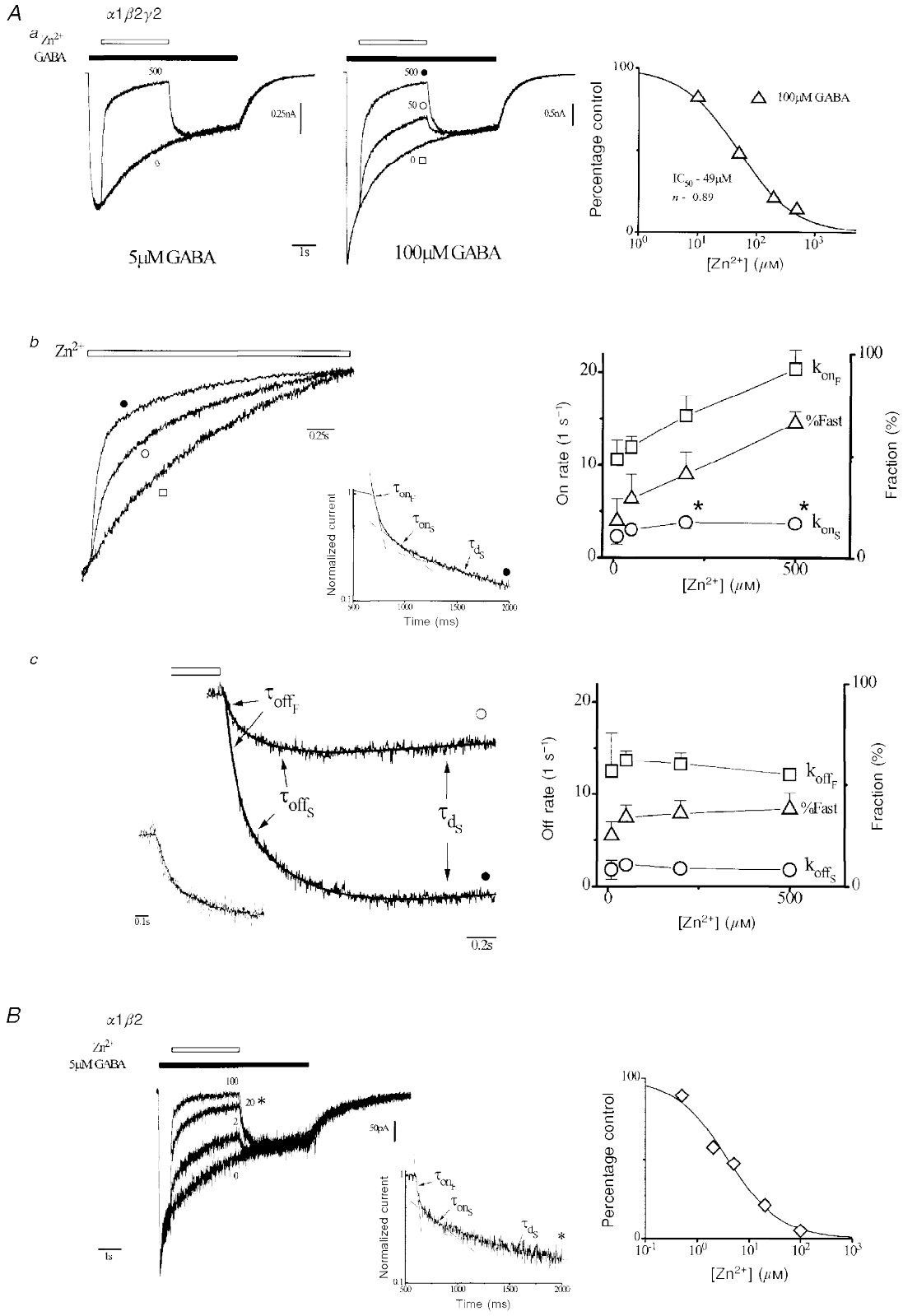

Figure 5. Zn^{2+} inhibition of currents previously activated by GABA

Aa, left panel, current response to Zn^{2+} application (500 μM, 3 s, open bar) from a cell expressing $\alpha1\beta2\gamma2$ receptors preactivated by low [GABA] (5 μM, filled bar). Zn^{2+} concentrations (in μM) are given adjacent to responses. Inhibition is determined at the end of the Zn^{2+} application. Middle panel, same protocol and cell at higher GABA concentration (100 μM) and over a range of Zn^{2+} concentrations. Vertical scaling was adjusted to nearly normalize current magnitude at the start of Zn^{2+} application. Right panel, current in Zn^{2+}, as percentage of control, *versus* Zn^{2+} concentration at indicated GABA concentration ($n = 5$). The

DISCUSSION

We investigated Zn^{2+} effects on GABA-triggered, Cl^- currents of recombinant $GABA_A$ receptors that differed in the γ2-subunit ($\alpha1\beta2$ and $\alpha1\beta2\gamma2$). We confirmed that receptors lacking the γ-subunit ($\alpha1\beta2$) manifest relative sensitivity and an apparent non-competitive mechanism (Draguhn *et al.* 1990; Smart *et al.* 1991). We then verified that receptors including the γ-subunit ($\alpha1\beta2\gamma2$) exhibit apparent competition (Chang *et al.* 1995) but because inhibition was incompletely surmounted by GABA we clarified the mechanism to be one of 'mixed antagonism' (Constanti, 1978). Rapid solution changes permitted analysis of the time course of macroscopic currents leading to the conclusion that Zn^{2+} distinctly modulates receptor gating. The findings suggested a state-dependent mechanism that selectively inhibits resting, $\alpha1\beta2$ receptors while preferentially affecting $\alpha1\beta2\gamma2$ states visited after ligand exposure. Subsequent studies involving selective Zn^{2+} delivery to resting or ligand-exposed receptors, and fluctuation analysis of $\alpha1\beta2\gamma2$ receptors provided additional support for this mechanism. Overall, the results support the idea that state-dependent Zn^{2+} inhibition is determined by the γ-subunit.

Mechanism of Zn^{2+} inhibition

It is likely that Zn^{2+} binds to a distinct extracellular site to allosterically induce transitions to a long-lived, non-conducting state(s) (Celentano *et al.* 1991; Smart, 1992). Our results from fluctuation analysis (Fig. 4) and the time course of inhibition (Fig. 5) support Zn^{2+}-mediated transitions to a non-conducting state(s) with slow closing rates (~10 s^{-1}). This rate is generally small compared with native gating (Macdonald, Rogers & Twyman, 1989) in accord with unchanged single-channel open times (Legendre & Westbrook, 1991; Smart, 1992). A new slow component in closed time histograms also supports distinct non-conducting states (Smart, 1992). Our analysis of the time course of macroscopic currents indicates two distinct non-conducting states (Figs 3 and 5). A single Zn^{2+} binding site is indicated by slope factors approaching 1 from our inhibition relationships and others (Mayer & Vyklicky, 1989; Celentano *et al.* 1991). Overall, a mechanism where Zn^{2+} binds to a single extracellular site and allosterically induces two kinetically distinct, non-conducting states reconciles these observations. This mechanism also accounts for mixed antagonism of $\alpha1\beta2\gamma2$ receptors (see below). Findings by others (Draguhn *et al.* 1990; Legendre & Westbrook, 1991; Smart, 1992) and us indicate that unitary current is unchanged, discounting rapid pore block. However, a pore-blocking mechanism (Draguhn *et al.* 1990) with slow binding kinetics cannot be excluded, but seems unlikely for three reasons: (1) multiple binding sites or other complex mechanisms are required to account for our kinetic data; (2) a ring of positive charge at the extracellular pore mouth (Schofield *et al.* 1987) would probably impede the entry of cations into the pore; and (3) weak or absent voltage dependence (Westbrook & Mayer, 1987; Mayer & Vyklicky, 1989; Draguhn *et al.* 1990; Smart & Constanti, 1990; Legendre & Westbrook, 1991; Celentano *et al.* 1991) indicates that the membrane electric field exerts little influence on inhibition, which is unlikely when ions enter and occlude the pore.

---

smooth curve is a fit of the inhibition equation ($IC_{50} = 49\ \mu M$, $S = 0{\cdot}89$). *Ab*, left, time courses of inhibition onset, normalized and replotted from *Aa* (symbols identify responses). Inset, onset time course normalized to unity and plotted on semilogarithmic axes (500 μM Zn^{2+}). Time course is well fitted by a triexponential function (smooth line; parameters: $A_{on_F} = 0{\cdot}38$, $k_{on_F} = 21\ s^{-1}$, $A_{on_S} = 0{\cdot}15$, $k_{on_S} = 6{\cdot}5\ s^{-1}$, $A_{d_S} = 0{\cdot}32$, $k_{d_S} = 1{\cdot}01\ s^{-1}$, $B = 0{\cdot}05$). The periods dominated by each exponential component are indicated by dashed lines labelled with associated time constants (reciprocal of respective rates: fast (τ_{on_F}) and slow (τ_{on_S}) inhibition onset and slow desensitization (τ_{d_S})). Right, concentration–response relationships for onset parameters derived from triexponential fitting (fast (k_{on_F}) and slow (k_{on_S}) onset rates, and fraction of onset that is fast [$\%\,Fast = 100A_{on_F}/(A_{on_F} + A_{on_S})$]). Asterisks mark k_{on_S}s that are significantly different ($P < 0{\cdot}05$, paired t test) from low Zn^{2+} (10 μM). *Ac*, time courses of inhibition recovery or offset replotted from *Aa* (symbols identify traces), shifted in magnitude to align current magnitude at the end of the Zn^{2+} application (open bar). Smooth lines are triexponential function fits (parameters are: 50 μM Zn^{2+}, $A_{off_F} = 0{\cdot}19$ nA, $k_{off_F} = 15{\cdot}4\ s^{-1}$, $A_{off_S} = 0{\cdot}36$ nA, $k_{off_S} = 2{\cdot}9\ s^{-1}$, $A_{d_S} = -0{\cdot}32$ nA, $k_{d_S} = 0{\cdot}47\ s^{-1}$, $B = -1{\cdot}26$ nA; 500 μM Zn^{2+}, $A_{off_F} = 0{\cdot}60$ nA, $k_{off_F} = 12{\cdot}2\ s^{-1}$, $A_{off_S} = 0{\cdot}63$ nA, $k_{off_S} = 1{\cdot}58\ s^{-1}$, $A_{d_S} = -0{\cdot}93$ nA, $k_{d_S} = 0{\cdot}61\ s^{-1}$, $B = -1{\cdot}20$ nA). Exponential components are labelled by associated time constants (reciprocal of respective rates: fast (τ_{off_F}) and slow (τ_{off_S}) inhibition onset and slow desensitization (τ_{d_S})). Inset, normalized offset time courses replotted on an expanded timescale (interrupted line, 50 μM Zn^{2+}; thick line, 500 μM Zn^{2+}). Right, concentration–response relationships for offset parameters (fast (k_{off_F}) and slow (k_{on_S}) offset rates, and fraction of offset that is fast (% Fast)) (generally $n = 5$). *B*, left, same protocol as in *Aa* applied to a cell expressing $\alpha1\beta2$ receptors. Inset, onset time course normalized to unity and plotted on semilogarithmic axes (20 μM Zn^{2+}). As with $\alpha1\beta2\gamma2$ receptors, time course is triexponential where each exponential component is indicated and labelled as in *Ab*. Right, current magnitude (% of control) *versus* Zn^{2+} concentration (generally $n = 5$) and fitted by inhibition equation (smooth curve, $IC_{50} = 3{\cdot}8\ \mu M$, $S = 0{\cdot}84$).

Proposed gating model for Zn^{2+} inhibition of $GABA_A$ receptors

We were interested in developing an explicit gating model that describes Zn^{2+} inhibition of $GABA_A$ receptors for three reasons. First, it permits quantitative evaluation of prospective gating mechanisms. Second, it provides insight into the interactions of multiple processes (agonist and antagonist binding, inhibition and gating) that govern receptor opening. Third, deep quantitative understanding is essential to consider possible physiological effects on postsynaptic GABAergic currents.

We began with a mechanism whereby Zn^{2+} binds to an extracellular site to trigger allosterically transitions to two kinetically distinct, non-conducting states, in accord with the above discussion. This mechanism, in the context of mixed antagonism exhibited by $\alpha1\beta2\gamma2$ receptors, is reminiscent of the 'mixed antagonistic model' proposed by Constanti (1978) and later refined by Smart & Constanti (1986) to account for picrotoxinin antagonism of GABA-triggered currents in crustacean muscle. Briefly in this model, agonist binds to two independent sites to trigger opening and antagonist binds to a single distinct site of each state with a unique dissociation constant. Antagonist-bound, conducting open receptors undergo a conformational change to a blocked, non-conducting state. The model describes state probabilities at equilibrium in terms of agonist and antagonist dissociation constants and a conformational constant specifying the ratio of conducting and blocked antagonist-bound open receptors. It elegantly accounts for non-competitive, uncompetitive and apparent competition (Smart & Constanti, 1986). The single antagonist binding site of this model is consistent with slope factors approaching 1 from our Zn^{2+} inhibition relationships and others (Mayer & Vyklicky, 1989; Celentano *et al.* 1991). We therefore adapted this formalism of open state inhibition to incorporate kinetics and two non-conducting states, yielding:

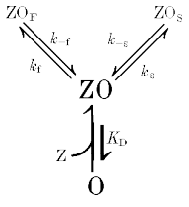

Scheme 1

where the open receptor (O) binds a single Zn^{2+} ion (Z) described by a dissociation constant (K_D) to achieve the bound open state (ZO). Through conformational changes, ZO passages to fast (ZO_F) or slow (ZO_S) non-conducting states governed by transition rate constants (k_f, k_{-f}, k_s, k_{-s}). We assumed that Zn^{2+} binding is rapid such that binding site occupation appears in continuous equilibrium relative to slower transitions involving ZO_F and ZO_S. Although speculative, other divalent ions may bind rapidly to ion channel proteins within milliseconds (Gurney, Tsien & Lester, 1987). We expanded gating Scheme 1 to a broader kinetic form that addresses activation, desensitization, and Zn^{2+} binding with all states resulting in:

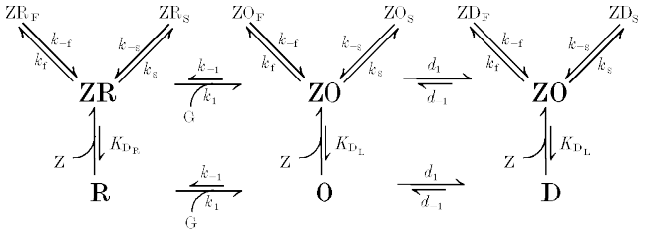

Scheme 2

The resting state (R) binds a single GABA molecule (G) governed by binding and unbinding rate constants (k_1 and k_{-1}), which leads to the conducting open state (O). This simple activation scheme reconciles the time course of empirical activation (see Fig. 2). O closes to the desensitized state (D) determined by transition rate constants (d_1 and d_{-1}). A single desensitized state approximates empirical desensitization. R, O or D bind a single Zn^{2+} ion leading to corresponding bound states (ZX, ZX_F and ZX_S where X = R, O or D) with the same transition rate constants (k_f, k_{-f}, k_s, k_{-s}). State-dependent binding arises from unique dissociation constants for R (K_{D_R}), and O or D (K_{D_L}). Transitions between Zn^{2+}-bound, resting-open and open-desensitized pairs are implied, although not explicitly shown, and are governed by the same rate constants that govern transitions between corresponding Zn^{2+}- free states since Zn^{2+} does not alter underlying native gating (see Fig. 5). Gating Scheme 2 is a first approximation of receptor function and is a simplification of complex $GABA_A$ receptor gating.

To begin quantitative evaluation of gating Scheme 2, we considered the time course of inhibition in $\alpha1\beta2\gamma2$ receptors (Fig. 5*Ab* and *Ac*) pre-exposed to a fully activating GABA concentration (100 μM). The unspecified parameters (k_1, k_{-1}, d_1, d_{-1}, K_{D_R}, K_{D_L}, k_f, k_{-f}, k_s, and k_{-s}) were determined. Rate constants governing activation ($k_1 = 100\ s^{-1}$ and $k_{-1} = 2\ s^{-1}$) and desensitization ($d_1 = 0{\cdot}4\ s^{-1}$, $d_{-1} = 0{\cdot}15\ s^{-1}$) were defined to cause roughly full receptor activation and approximate empirical time courses (Figs 2*B* and 5*Aa*). Gating Scheme 2 dictates that inhibition offset is biexponential with rates identical to reverse rate constants. Therefore these were set nearly equal to experimental offset rates ($k_{-f} = 12\ s^{-1}$ and $k_{-s} = 2\ s^{-1}$). To approximate the intrinsic filtering of our measurement system we applied a first order filter (−3 dB, 10 Hz) to model currents. K_{D_R} was set to infinity, since Zn^{2+} interactions with resting receptors are probably small under these conditions. The remaining unspecified parameters (K_{D_L}, k_f and k_s) were estimated using target time courses comprised of inhibition onset and offset at two Zn^{2+} concentrations (50 and 500 μM) computed from mean parameters (Fig. 5*Ab* and *Ac*) and combined with model desensitization. The resultant estimated parameters ($K_{D_L} = 328\ \mu$M, $k_f = 17{\cdot}1\ s^{-1}$ and $k_s = 7{\cdot}3\ s^{-1}$) completely specified gating Scheme 2.

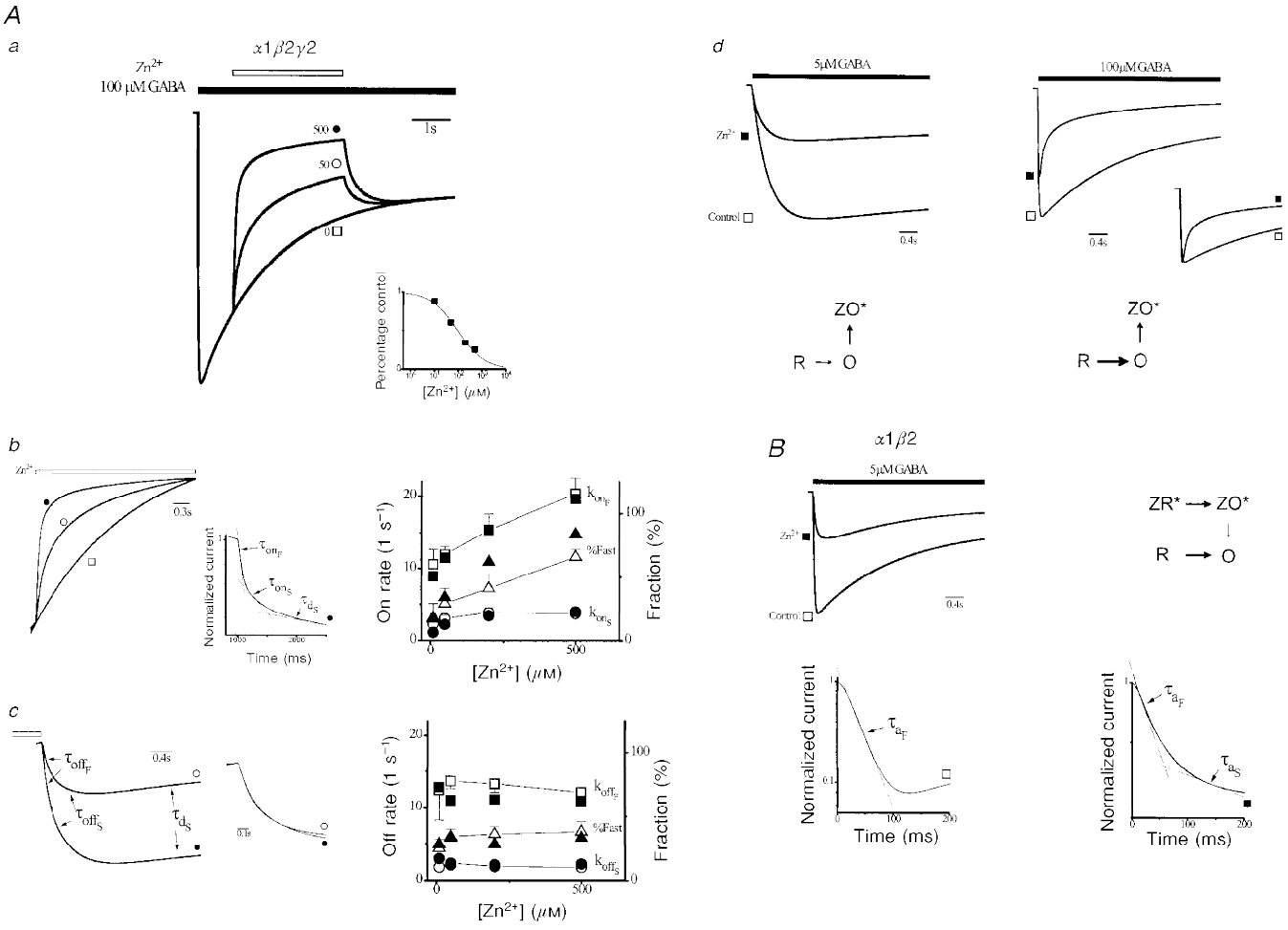

Figure 6. Responses from gating models

Aa, responses from $\alpha1\beta2\gamma2$ gating model (see text) to Zn^{2+} application (open bar, concentrations adjacent to response in μM) of currents preactivated by GABA (filled bar). Inset, current in Zn^{2+}, as percentage of control, *versus* Zn^{2+} concentration and the fit by the inhibition equation (smooth curve, $IC_{50} = 94\ \mu M$, $S = 0{\cdot}77$). *Ab*, left, normalized time courses of inhibition onset replotted from *Aa* (symbols identify responses). Middle, onset time course normalized to unity and plotted on semilogarithmic axes (500 μM Zn^{2+}). Time course is triexponential with each component indicated by dashed straight lines labelled with associated time constants (reciprocal of respective rates: fast (τ_{on_F}) and slow (τ_{on_S}) inhibition onset and slow desensitization (τ_{d_S})). Superimposed line is fitted by a triexponential function (parameters: $A_{on_F} = 0{\cdot}47$, $k_{on_F} = 18\ s^{-1}$, $A_{on_S} = 0{\cdot}16$, $k_{on_S} = 2{\cdot}5\ s^{-1}$, $A_{d_S} = 0{\cdot}17$, $k_{d_S} = 0{\cdot}22\ s^{-1}$, $B = 0{\cdot}04$). Right, concentration–response relationships for fitted parameters from gating model (filled symbols) and empirical responses replotted from Fig. 5*Ab* (open symbols). *Ac*, time courses of inhibition offset replotted from *Aa*, shifted in magnitude to align currents at the end of the Zn^{2+} application (open bar). Time courses are well fitted by a triexponential with each component labelled by the associated time constant (reciprocal of respective rates: fast (τ_{off_F}) and slow (τ_{off_S}) inhibition onset and slow desensitization (τ_{d_S})). Middle, normalized offset time courses replotted on an expanded time scale. Right, concentration–response relationships for offset parameters from gating model (filled symbols) and empirical responses replotted from Fig. 5*Ac* (open symbols). *Ad*, $\alpha1\beta2\gamma2$ model responses triggered at low (5 μM) and high (100 μM) GABA concentrations (bar) in control (□) and in constant Zn^{2+} (300 μM, ■) with vertical scaling adjusted to normalize for peak control currents. Dominant model gating pathways are shown below responses where rate magnitudes are related to the emboldening and length of transition arrows and ZX* represents Zn^{2+}-bound states (ZX, ZX_S and ZX_F) associated with state X (X = R, O, or D). *B*, $\alpha1\beta2$ model responses at 5 μM GABA (bar) in control (□) and in the presence of Zn^{2+} (10 μM, ■) with dominant model gating pathways shown adjacently. Below, semilogarithmic plot of onset time courses from above normalized to peak current magnitude. In control, activation is described by a single fast exponential (dashed line, time constant, τ_{a_F}). Zn^{2+} adds a second slow exponential component to activation (time constant, τ_{a_S}). The sum of the fitted triexponentials (superimposed line; $A_{on_F} = 0{\cdot}31$, $k_{on_F} = 19\ s^{-1}$, $A_{on_S} = 0{\cdot}11$, $k_{on_S} = 3{\cdot}4\ s^{-1}$, $A_{d_S} = -0{\cdot}31$, $k_{d_S} = 0{\cdot}54\ s^{-1}$, $B = 0{\cdot}87$) describes the activation time course (see text).

Figure 6*Aa* shows the effects of Zn^{2+} application on preactivated responses of gating Scheme 2. Zn^{2+} reversibly inhibits current in a dose-dependent fashion. These responses and the concentration–response relationship (inset) are strikingly similar to our experimental results (see Fig. 5*Aa–c*). Zn^{2+} enhanced the speed of inhibition onset (Fig. 6*Ab*, left) with a biexponential time course (middle). Figure 6*Ac*, left panel, shows inhibition offset time courses replotted from Fig. 6*Aa* after shifting to align currents at the end of the Zn^{2+} application (open bar). The time courses are triexponential and the normalized early offset time course is unaffected by Zn^{2+}. Figure 6*Ab* and *c*, right panels, plot model and experimental concentration–response relationships of fitted onset and offset parameters. Overall, gating Scheme 2 provides a remarkably close accounting of empirical Zn^{2+} inhibition of preactivated $\alpha1\beta2\gamma2$ receptors. Therefore, this model describes the dominant gating governing inhibition of macroscopic currents.

We next examined gating Scheme 2 for our empirical observations of $\alpha1\beta2\gamma2$ receptors in constant Zn^{2+} (Fig. 2*B*). The value of K_{D_R} was computed to be 8600 μM, which assumed that the magnitude of insurmountable inhibition (Fig. 1*B*) reflects inhibited resting receptors. Figure 6*Ad*, top left panel, shows responses of gating Scheme 2 triggered by low GABA concentration in control and in Zn^{2+}. The control response activates and desensitizes slowly.

Zn^{2+} depresses peak current more than twofold without appreciably changing gating. The scheme in Fig. 6*Ad* shows the dominant gating pathways of the model in Zn^{2+}. Slow activation (R→O) permits faster inhibition (O→ZO*), renders receptors non-conducting rapidly, and prevents accumulation of O states thereby depressing peak current. Figure 6*Ad*, top right panel, shows model responses for the same protocol but at high GABA concentration. Activation and desensitization are accelerated in control. Current inhibition is reduced marking antagonism, and desensitization is accelerated (inset). Accelerated activation causes rapid accumulation of O states before inhibition thereby increasing peak. Apparent desensitization is enhanced owing to increased receptor closing by inhibition following current peak. These results demonstrate that gating Scheme 2 qualitatively reproduces apparent competitive antagonism and gating effects of $\alpha1\beta2\gamma2$ receptors.

Both the results and the structure of gating Scheme 2 support the argument that mixed antagonism of $\alpha1\beta2\gamma2$ receptors results from the kinetic interplay of inhibition of ligand-exposed receptors and GABA-triggered activation. Furthermore, the temporal relationship of agonist and antagonist presentation may play a critical role in the apparent mechanism of antagonism. Antagonism can appear non-competitive when the antagonist is presented after agonist exposure or mixed when pre- or coapplied.

We next considered whether gating Scheme 2 could account for the distinct Zn^{2+} effects on $\alpha1\beta2$ receptors. Gating Scheme 2 application to $\alpha1\beta2$ receptors is justified because, as with $\alpha1\beta2\gamma2$ receptors, inhibition is state dependent and involves two kinetically distinct states. $\alpha1\beta2$ receptors exhibit faster activation, preferential inhibition of resting receptors, and overall greater sensitivity to Zn^{2+}. Therefore, we revised only the activation rate constant (k_1), and both dissociation constants (K_{D_R} and K_{D_L}). k_1 was set to 50 s^{-1}, consistent with empirical activation triggered by 5 μM GABA (Fig. 2*A*). The value of K_{D_R} was computed to be 3·5 μM based on the IC_{50} in constant Zn^{2+} (Fig. 1*A*) and the assumption that inhibition reflects blocked resting receptors. Comparable inhibition of preactivated $\alpha1\beta2$ receptors requires about a tenfold reduction in Zn^{2+} concentration relative to $\alpha1\beta2\gamma2$ (see Fig. 5). Therefore, we simply reduced K_{D_L} in the $\alpha1\beta2\gamma2$ model (328 μM) tenfold for $\alpha1\beta2$ (33 μM). Gating Scheme 2 with these three redefined parameters became the gating model for $\alpha1\beta2$ receptors. In control, $\alpha1\beta2$ gating model activation is rapid and accompanied by appreciable desensitization (Fig. 6*B*, top panel). Zn^{2+} reduces peak current and slows both activation and apparent desensitization kinetics. Activation time course is monoexponential in control. Zn^{2+} induces a second slower exponential (Fig. 6*B*, lower panel). Therefore, the $\alpha1\beta2$ gating model qualitatively reproduces the effects of Zn^{2+} on $\alpha1\beta2$ gating. The top panel of Fig. 6*B* shows the dominant gating in Zn^{2+} where the fast activation arises from resting unbound channels (R→O). The slow component results from two sequential transitions. Zn^{2+}-bound receptors first undergo activation (ZR*→ZO*) that is followed by slow Zn^{2+} unbinding and subsequent receptor conduction (ZO*→O). Slowed desensitization arises from the resultant reduction in open state probability.

Gating Scheme 2 reproduces the kinetics and magnitude of Zn^{2+} inhibition of $\alpha1\beta2\gamma2$ receptors previously activated by GABA. In constant Zn^{2+}, it accounts for the primary effects on current magnitude and kinetics of both $\alpha1\beta2$ and $\alpha1\beta2\gamma2$ receptors. Gating Scheme 2 comprehensively accounts for our primary empirical findings and therefore can be considered as a general mechanism for Zn^{2+} inhibition of $GABA_A$ receptors when determination of state-dependent Zn^{2+} binding by the γ-subunit is included. This general mechanism serves to unify our understanding of Zn^{2+} inhibition of $GABA_A$ receptors by accounting for the diversity of observed Zn^{2+} effects.

Comparison with other studies

Our results in $\alpha1\beta2\gamma2$ receptors are in accord with similar recombinant investigations and reports from *ex vivo* receptors from hippocampus and spinal cord that are probably $\alpha\beta\gamma$ receptors (Persohn, Malherbe & Richards, 1991; Wisden, Laurie, Monyer & Seeburg, 1992). Legendre & Westbrook (1991) investigated Zn^{2+} inhibition of GABA-triggered currents in rat cultured hippocampal neurons and found that inhibition of preactivated receptors appeared non-competitive. The activation time course was unchanged by Zn^{2+} coapplication at low GABA concentration (5 μM). At higher GABA concentrations, Zn^{2+} enhanced a fast

component of apparent desensitization without affecting a slow component. Coapplication resembles our experiments in constant Zn^{2+} since Zn^{2+} is present at the time of GABA application. The authors concluded that Zn^{2+} rapidly acts on states leading up to channel opening (monoliganded and doubly liganded states). Celentano *et al.* (1991) reported that GABA incompletely surmounted inhibition of GABA-triggered currents caused by coapplied Zn^{2+} in cultured chick spinal cord neurons. White & Gurley (1995) have reported similar observations in $\alpha\beta\gamma$ receptors expressed in *Xenopus* oocytes where Zn^{2+} was applied before GABA. These results and those regarding non-competitive inhibition of preactivated receptors above are reconciled by our general mechanism for receptors containing a γ-subunit.

Our observation of apparent non-competition in $\alpha1\beta2$ receptors agrees with previous reports in recombinant $\alpha\beta$ receptors (Draguhn *et al.* 1990; Smart *et al.* 1990), rat superior cervical ganglion (Smart & Constanti, 1990) and lobster muscle (Smart & Constanti, 1982).

Yakushiji *et al.* (1987) investigated GABA-triggered currents in frog dorsal root ganglion (DRG) using rapid perfusion techniques. Zn^{2+} inhibition was completely antagonized by GABA in coapplication experiments suggesting a competitive mechanism that disagrees with our results in $\alpha1\beta2\gamma2$ receptors and constant Zn^{2+}. Our general mechanism suggests that for $\alpha1\beta2\gamma2$ receptors, inhibition of peak current is due to kinetic interactions of inhibition and activation. Activation kinetics are divergent in frog DRG (Akaike *et al.* 1987) and mammalian receptors (Legendre & Westbrook, 1991; Maconochie *et al.* 1994; our Fig. 2), which manifest biexponential and monoexponential time courses, respectively. Therefore, although ligand-exposed receptors may bind Zn^{2+} preferentially, differences in the activation pathway in DRG at high GABA concentration may prevent appreciable receptor inhibition before current peak. At the same time, Zn^{2+} accelerated the fast phase of apparent desensitization, which is inconsistent with simple competitive antagonism but in accord with our results.

Zn^{2+} also inhibits currents from a novel class of GABA receptors ($GABA_C$) identified in the retina (Feigenspan, Wassle & Bormann, 1993), which is probably a homomer of ρ-subunits that share 30–38% sequence homology with $GABA_A$ receptor subunits. Native $GABA_C$ receptors as well as those resulting from ρ-subunit expression (Calvo, Vazquez & Miledi, 1994; Chang *et al.* 1995) exhibit mixed antagonism. Chang *et al.* (1995) proposed that this is due to either different affinities of agonist-free and agonist-bound receptors or two distinct sites, competitive and non-competitive. The former mechanism is consistent with our proposed general mechanism.

Possible structural underpinnings of Zn^{2+} binding site

What are the possible structural underpinnings of an extracellular Zn^{2+} binding site? Studies of Zn^{2+}-interacting proteins have shown that binding can be co-ordinated by Cys, His, Glu and/or Asp residues in a ternary combination (Vallee & Auld, 1990). Recent work by Wang, Hackam, Guggino & Cutting (1995) has identified a histidine residue (H156) on the $\rho1$-subunit that is critical for Zn^{2+} inhibition of $GABA_C$ receptors. Figure 7 shows that this residue is distal to the cysteine loop on the extracellular amino

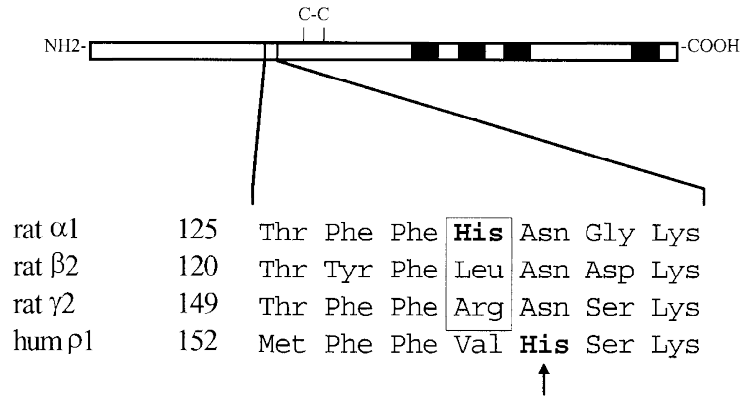

Figure 7. Amino acid sequences

Above, cartoon of the general primary structure of $GABA_A$ receptor subunits showing amino and carboxy termini, and four transmembrane spanning regions (shaded). The extracellular amino domain contains a cysteine loop (C-C). Lines indicate approximate location of amino acid sequences shown below. Region of protein involved in co-ordinating Zn^{2+} binding is putatively extracellular. Below, comparison of amino acid sequences of $GABA_A$ receptor subunits with homologous residues in the neighborhood of a $\rho1$ histidine (156) on extracellular amino terminus that is critical to Zn^{2+} inhibition of $GABA_C$ receptors (Wang *et al.* 1995). Amino acids are in three letter code and numbers refer to the codons of the predicted amino acid sequence of the full-length cDNA where the canonical methionine is codon 1. Arrow marks the location of the critical histidine (emboldened) of $\rho1$. Box encloses adjoining location on $GABA_A$ subunits that contains a histidine (emboldened) residue on the $\alpha1$-, a neutral leucine on $\beta2$-, and a positively charged arginine on the $\gamma2$-subunit.

domain of the ρ1-subunit. In this region there is high homology among $GABA_A$ receptor α, β, γ and ρ1-subunits. The α-subunit has a histidine in an adjacent location (His128). Perhaps His128 contributes to the Zn^{2+} binding pocket of $GABA_A$ receptors in a manner similar to His156 in $GABA_C$. A permissive leucine (Leu123) or a nearby enhancing aspartate (Asp125) of the β-subunit could complete a high-affinity, binding pocket for resting $\alpha\beta$ receptors. Reduced affinity of resting $\alpha1\beta2\gamma2$ receptors could arise from the arginine (Arg149) of the γ-subunit that would be protonated (pK_R, $-12{\cdot}48$) at physiological pH and positively charged. This may reduce the affinity through electrostatic repulsion or interference with Zn^{2+} interactions with His128. These speculations will need to be verified with site-directed mutagenesis.

A key observation of this study is the dependence of Zn^{2+} inhibition on receptor state. State dependence of binding pocket affinity can be envisaged based on conformational changes observed in the homologous nicotinic acetylcholine receptor (nAChR; Schofield *et al.* 1987). Electron crystallography of resting and activated nAChRs indicates ligand binding triggers up to 28 deg of counter-clockwise rotation of the extracellular domains (Unwin, 1995). This could cause relative rearrangement of amino domains, change the Zn^{2+} binding pocket, and lead to altered affinity. Such conformational changes may account for the state dependence of binding for both receptors.

With these results we conclude that Zn^{2+} inhibition of $GABA_A$ receptors is a subunit-dependent mechanism whereby Zn^{2+} selectively inhibits resting receptors in the absence of the γ-subunit and ligand-exposed receptors when present. We further propose a general model of inhibition in which Zn^{2+} binds rapidly to a single extracellular site that allosterically induces two non-conducting states, site affinity is state dependent, and the features of state dependence are determined by the γ-subunit. This general mechanism appears to unify the understanding of Zn^{2+} inhibition through its ability to account for a diversity of reported Zn^{2+} effects. The results also extend, in general, insight into the interactions of gating, agonist and antagonist binding of ligand-gated ion channels.

Akaike, N., Yakushiji, T., Tokutomi, N. & Carpenter, D. O. (1987). Mulitiple mechanisms of antagonism of γ-aminobutyric-acid (GABA) responses. *Cellular and Molecular Neurobiology* **7**, 97–103.

Aniksztejn, L., Charlton, G. & Ben-Ari, Y. (1987). Selective release of endogenous zinc from the hippocampal mossy fibers *in situ*. *Brain Research* **404**, 58–64.

Assaf, S. Y. & Chung, S. H. (1984). Release of endogenous Zn^{2+} from brain tissue during activity. *Nature* **308**, 734–738.

Burkat, P. M., Roberts, W. & Gingrich, K. J. (1995). Gamma subunit influences the mechanism of zinc inhibition in recombinant $GABA_A$ receptors. *Journal of Neuroscience* **21**, A850.

Calvo, D. J., Vazquez, A. E. & Miledi, R. (1994). Cationic modulation of rho1 type gamma-aminobutyrate receptors expressed in *Xenopus* oocytes. *Proceedings of the National Academy of Sciences of the USA* **91**, 12725–12729.

Celentano, J. J., Gyenes, M., Gibbs, T. T. & Farb, D. H. (1991). Negative modulation of the γ-aminobutyric acid response by extracellular zinc. *Molecular Pharmacology* **40**, 766–773.

Chang, Y., Amin, J & Weiss, D. S. (1995). Zinc is a mixed antagonist of homomeric $\rho1$ γ-aminobutryic acid-activated channels. *Molecular Pharmacology* **47**, 595–602.

Constanti, A. (1978). The 'mixed' effect of picrotoxin on the GABA dose/conductance relation recorded from lobster muscle. *Neuropharmacology* **17**, 159–167.

Curtis, D. R. & Gynther, B. D. (1987). Divalent cations reduce depolarization of primary afferent termination by GABA. *Brain Research* **422**, 192–195.

Draguhn, A., Verdoorn, T. A., Ewert, M., Seeburg, P. H. & Sakmann, B. (1990). Functional and molecular distinction between recombinant rat $GABA_A$ receptor subtypes by Zn^{2+}. *Neuron* **5**, 781–788.

Feigenspan, A., Wassle, H. & Bormann, J. (1993). Pharmacology of GABA receptor Cl^- channels in rat retinal bipolar cells. *Nature* **361**, 159–161.

Frederickson, C. J. & Moncrieff, D. W. (1994). Zinc containing neurons. *Biological Signals* **3**, 127–130.

Gingrich, K. J., Roberts, W. A. & Kass, R. S. (1995). Dependence of the $GABA_A$ receptor gating kinetics on the γ-subunit isoform: implications for structure–function relations and synaptic transmission. *Journal of Physiology* **489**, 529–543.

Gurney, A. M., Tsien, R. Y. & Lester, H. A. (1987). Activation of a potassium current by rapid photochemically generated step increases of intracellular calcium in rat sympathetic neurons. *Proceedings of the National Academy of Sciences of the USA* **84**, 3496–3500.

Hamill, O. P., Marty, A., Neher, E., Sakmann, B. & Sigworth, F. J. (1981). Improved patch-clamp techniques for high-resolution current recording from cells and cell-free membrane patches. *Pflügers Archiv* **391**, 85–100.

Haug, F.-M. S. (1967). Electron microscopical localization of the zinc in hippocampal mossy fibre synapses by a modified silver procedure. *Histochemie* **8**, 355–368.

Howell, G. A., Welch, M. G. & Frederickson, C. J. (1984). Stimulation-induced uptake and release of zinc in hippocampal slices. *Nature* **308**, 736–738.

Legendre, P. & Westbrook, G. L. (1991). Noncompetitive inhibition of γ-aminobutyric $acid_A$ channels by Zn. *Molecular Pharmacology* **39**, 267–274.

Levitan, E. S., Schofield, P. R., Burt, D. R., Rhee, L. M., Wisden, W., Kohler, M. M., Fujita, N., Rodriguez, H. F., Stephenson, F. A., Darlison, M. G., Barnard, E. A. & Seeburg, P. H. (1988). Structural and functional basic for $GABA_A$ receptor heterogeneity. *Nature* **335**, 76–79.

Macdonald, R. L., Rogers, C. J. & Twyman, R. E. (1989). Kinetic properties of the $GABA_A$ receptor main-conductance state of mouse spinal cord neurons in culture. *Journal of Physiology* **410**, 479–499.

Maconochie, D. J., Zempel, J. M. & Steinbach, J. H. (1994). How quickly can $GABA_A$ receptors open? *Neuron* **12**, 61–71.

Mayer, M. L. & Vyklicky, L. Jr (1989). The action of zinc on synaptic transmission and neuronal excitability in cultures of mouse hippocampus. *Journal of Physiology* **415**, 351–365.

Neher, E. & Stevens, C. F. (1977). Conductance fluctuations and ionic pores in membranes. *Annual Reviews Biophysics and Bioengineering* **6**, 345–381.

Perez-Clausell, J. & Danscher, G. (1985). Intravesicular localization of zinc in rat telencephalic boutons. A histochemical study. *Brain Research* **337**, 91–98.

Persohn, E., Malherbe, P. & Richards, J. G. (1991). *In situ* hybridization histochemistry reveals a diversity of $GABA_A$ receptor subunit mRNA's in neurons of rat spinal cord and dorsal root ganglia. *Journal of Neuroscience* **42**, 497–507.

Puia, G., Santi, M., Vicini, S., Pritchett, D., Pardy, R., Paul, S., Seeburg, P. & Costa, E. (1990). Neurosteroids act on recombinant human $GABA_A$ receptors. *Neuron* **4**, 759–765.

Saxena, N. C. & Macdonald, R. L. (1994). Assembly of $GABA_A$ receptor subunits: role of the γ-subunit. *Journal of Neuroscience* **14**, 7077–7086.

Schofield, P. R., Darlison, M. G., Fujita, N., Burt, D. R., Stephenson, F. A., Rodriguez, H., Rhee, L. M., Ramachandran, J., Reale, V., Glencorse, T. A., Seeburg, P. H. & Barnard, E. A. (1987). Sequence and functional expression of the $GABA_A$ receptor shows a ligand-gated receptor super-family. *Nature* **328**, 221–227.

Sigel, E., Baur, R., Mohler, H. & Malherbe, P. (1990). The effect of subunit composition of rat brain $GABA_A$ receptors on channel function. *Neuron* **5**, 703–711.

Smart, T. G. (1992). A novel modulatory binding site for zinc on the $GABA_A$ receptor complex in cultured rat neurones. *Journal of Physiology* **447**, 587–625.

Smart, T. G. & Constanti, A. (1982). A novel effect of zinc on the lobster muscle GABA receptor. *Proceedings of the Royal Society* B **215**, 327–341.

Smart, T. G. & Constanti, A. (1986). Studies on the mechanism of action of picrotoxinin and other convulsants at the crustacean muscle GABA receptor. *Proceedings of the Royal Society* B **227**, 191–216.

Smart, T. G. & Constanti, A. (1990). Differential effects of zinc on the vertebrate GABA-receptor complex. *British Journal of Pharmacology* **99**, 643–654.

Smart, T. G., Moss, S. J., Xie, X. & Huganir, R. L. (1991). $GABA_A$ receptors are differentially sensitive to zinc: dependence on subunit composition. *British Journal of Pharmacology* **103**, 1837–1839.

Smart, T. G., Xie, X. & Krishek, B. J. (1994). Modulation of inhibitory and excitatory amino acid recpetor ion channels by zinc. *Progress in Neurobiology* **42**, 393–441.

Unwin, N. (1995). Acetylcholine receptor imaged in the open state. *Nature* **373**, 37–43.

Vallee, B. L. & Auld, D. S. (1990). Zinc coordination, function and structure of zinc enzymes and other proteins. *Biochemistry* **29**, 5647–5659.

Verdoorn, T. A., Draguhn, A., Ymer, S., Seeburg, P. H. & Sakmann, B. (1990). Functional properties of recombinant rat $GABA_A$ receptors depend on subunit composition. *Neuron* **4**, 919–928.

Wang, T. L., Hackam, A., Guggino, W. B. & Cutting, G. R. (1995). A single histidine residue is essential for zinc inhibtion of GABA rho 1 receptors. *Journal of Neuroscience* **15**, 76841–76891.

Westbrook, G. L. & Mayer, M. L. (1987). Micromolar concentrations of Zn^{2+} antagonize NMDA and GABA responses of hippocampal neurons. *Nature* **328**, 640–643.

White, G. & Gurley, D. A. (1995). γ-Subunits influence Zn block of $\gamma 2$ containing $GABA_A$ receptor currents. *NeuroReport* **6**, 461–464.

Wisden, W., Laurie, D. J., Monyer, H. & Seeburg, P. H. (1992). The distribution of 13 $GABA_A$ receptor subunit mRNAs in the rat brain I. telencephalon, diencephalon, mesencephalon. *Journal of Neuroscience* **12**, 1040–1062.

Xie, X. M. & Smart, T. G. (1991). A physiological role for endogenous zinc in rat hippocampal synaptic neurotransmission. *Nature* **349**, 521–524.

Yakushiji, T., Tokutomi, N., Akaike, N. & Carpenter, D. O. (1987). Antagonists of GABA responses, studied using internally perfused frog dorsal root ganglion neurons. *Neuroscience* **22**, 1123–1133.

Zhou, F. M. & Hablitz, J. J. (1993). Zinc enhances GABAergic transmission in rat neocortical neurons. *Journal of Neurophysiology* **70**, 1264–1269.

Acknowledgements

We thank Larry Wagner II for preparation of cultured cells and their transient transfection. This work was supported by a Whitaker Foundation research grant to K.J.G.

Corresponding author

K. J. Gingrich: Department of Anesthesiology, University of Rochester, School of Medicine, 601 Elmwood Avenue, Rochester, NY, 14642, USA.

Email: kgingrich@ccmail.anes.rochester.edu